

Research paper

## Traveling chimera states in continuous media

A.J. Alvarez-Socorro<sup>a,b,\*</sup>, M.G. Clerc<sup>a</sup>, N. Verschueren<sup>c</sup>

<sup>a</sup> Departamento de Física and Millennium Institute for Research in Optics, Facultad de Ciencias Físicas y Matemáticas, Universidad de Chile, Casilla Santiago, 487-3, Chile

<sup>b</sup> Laboratorio de Investigación, Desarrollo e Innovación, Zenta Group, Andrés Bello 2687, Las Condes, Santiago, Chile

<sup>c</sup> College of Engineering, Mathematics and Physical Sciences, University of Exeter, Exeter, United Kingdom



### ARTICLE INFO

*Article history:*

Received 4 February 2020

Revised 23 September 2020

Accepted 2 October 2020

Available online 6 October 2020

*Keywords:*

Localized structures

Chimeras

Nonvariational effects

Traveling states

### ABSTRACT

Coupled oscillators exhibit intriguing dynamical states characterized by the coexistence of coherent and incoherent domains known as chimera states. Similar behaviors have been observed in coupled systems and continuous media. Here we investigate the transition from motionless to traveling chimera states in continuous media. Based on a prototype model for pattern formation, we observe coexistence between motionless and traveling chimera states. The spatial disparity of chimera states allows us to reveal the motion mechanism. The propagation of chimera states is described by their median and centroidal point. The mobility of these states depends on the size of the incoherent domain. The bifurcation diagram of traveling chimeras is elucidated.

© 2020 Elsevier B.V. All rights reserved.

## 1. Introduction

In recent years the so-called chimera states, defined as dynamical behaviors having coexistence of coherent and incoherent domains, have attracted the attention of the scientific community [1–22]. Since the seminal work of Kuramoto and Battogtokh [2], the universal phenomenon of chimeras states has been intensively studied. Most of these studies focus on discrete systems of coupled oscillators and only recently the dynamical richness of chimera solutions in continuous models has been explored [23,24,26,27]. In continuous media, the chimera states can be understood as localized spatiotemporal complex patterns resulting from a symmetry breaking. These localized structures can be of spatiotemporal chaotic, chaotic, or quasi-periodic nature. Experimentally, these states were reported in a liquid crystal light valve with optical feedback (termed *Chaoticons* [23,24]) and in fluids (identified as localized turbulence [28]). A requirement for observing chimera states in continuous media is the coexistence between a chaotic spatiotemporal or quasi-periodic pattern and a homogeneous state. The origin by which the domains are blocked is because the pattern in the interfaces induces a barrier, *pinning effect* [23,24,29]. As a result of this mechanism, one expects to find a family of localized solutions organized through a snaking type bifurcation diagram [30]. The discrete counterpart of the snaking type bifurcation diagram for chimera states has also been reported [15–18].

Experimentally, chimera states have been observed in discrete coupled systems in the following contexts: chemical oscillators [4], neurodynamics [19], liquid crystals [5], optoelectronic delayed feedback setup [20], laser diode coupled to a non-linear saturable absorber [21], and laser diode subjected to a coherent polarization [22], among others. Chimera solutions

\* Corresponding author at: Departamento de Física and Millennium Institute for Research in Optics, Facultad de Ciencias Físicas y Matemáticas, Universidad de Chile, Casilla 487-3, Santiago, Chile.

E-mail address: [alejandro.alvarez@ing.uchile.cl](mailto:alejandro.alvarez@ing.uchile.cl) (A.J. Alvarez-Socorro).

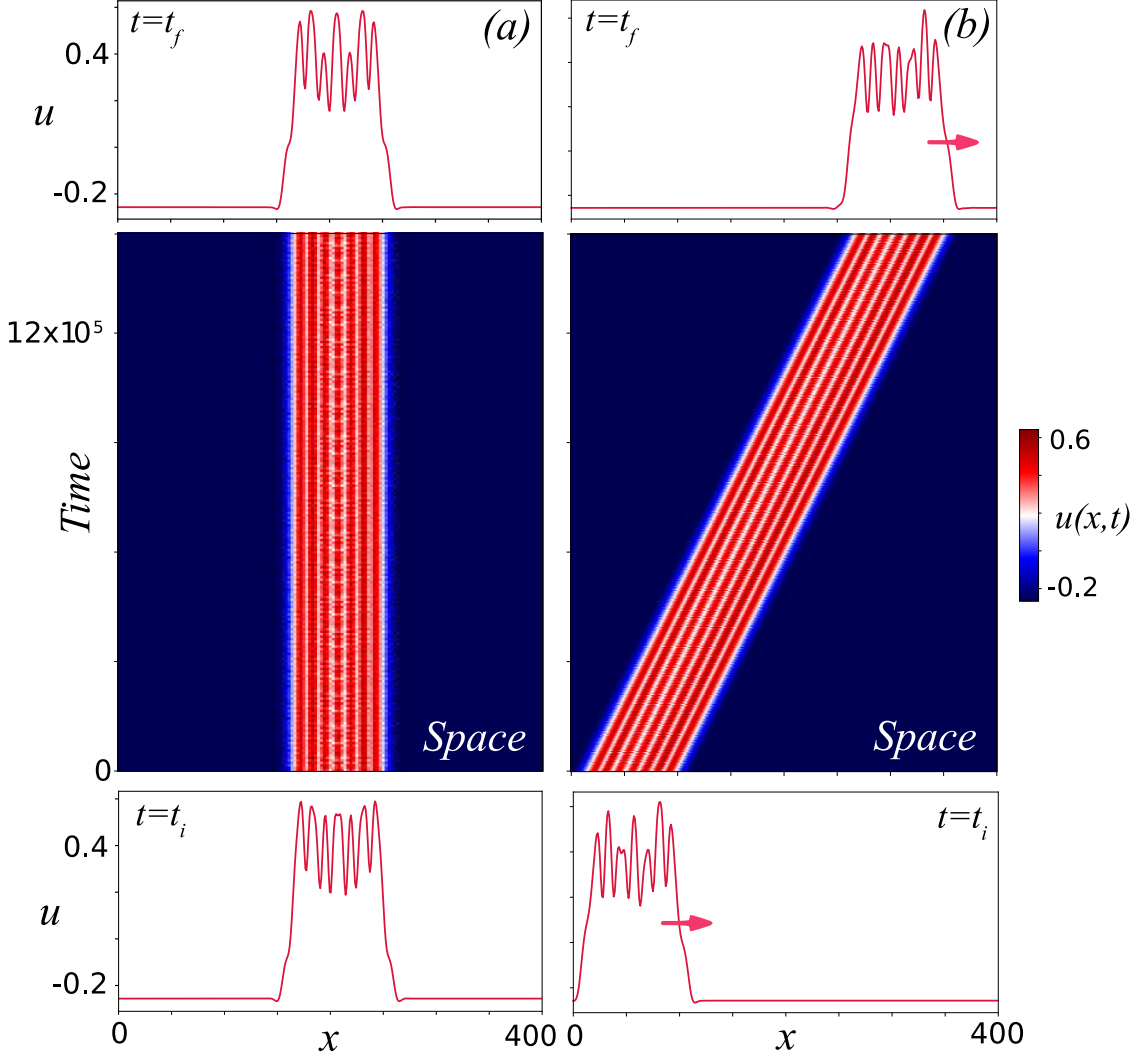


**Fig. 1.** (color online) Coexisting motionless and traveling chimera states. Spatiotemporal diagram of motionless (a) and traveling chimera state (b) for Eq. (1) when  $\eta = -0.04$ ,  $\mu = -0.09$ ,  $v = 1$ ,  $b = -1.5$ , and  $c = 10$ . The top and bottom panels account for the profiles of the chimera state at the initial  $u(x, t = t_i = 0)$  and final  $u(x, t = t_f = 15 \times 10^5)$  instant of the spatiotemporal diagram.

can be interpreted as particle-type solutions; that is, these solutions can be characterized by a set of continuous parameters such as the position and width. They can be motionless [3], propagative [31–33], or wandering [34] in their position or centroid. The localized structures can move as a result of external symmetry-breaking instability induced by a phase gradient [35], off-axis feedback [36], resonator detuning [37], and space-delayed feedback [38]. Likewise, internal symmetry-breaking instability can induce propagative localized states [39,40]. Indeed, when a parameter is modified in continuous media, localized solutions become asymmetric and propagate due to non-variational effects. The dynamics of localized states can be described by the median and centroid. The median is defined as the middle point of the incoherent (spatiotemporal) domain. Meanwhile, the centroid is the point defined by the profile weighted average of the localized state. In general, for asymmetric solutions, both quantities do not coincide. The difference between these quantities accounts for the disparity.

In this manuscript, we aim to investigate traveling chimera states in continuous media. Fig. 1 illustrates, for the same parameters, a motionless and traveling chimera state. Using a prototype model for pattern formation, the non-variational Turing-Swift-Hohenberg equation, we unveil the transition of chimera states from motionless to propagative. Since this transition is subcritical, depending on the initial conditions the system would exhibit coexistence between chimera states of different sizes and speeds. Indeed, a family of propagative chimera states and their respective bifurcation diagram is presented. The motion mechanism of chimera states can be characterized using their spatial disparity. Notice that in spite of their spatiotemporal chaotic nature, traveling chimera states propagate with a well-defined oscillatory speed.

The rest of the article is organized as follows. In Section 2, the mathematical model for pattern formation used throughout the paper as well as their chimera solutions are introduced. Section 3 presents a characterization of chimera solutions in

terms of the temporal evolution of their centroid, median, and disparity. Section 4 is devoted to the study of the propagation of chimera states as a function of their width. Concluding remarks are presented in Section 5.

## 2. The non-variational Turing-Swift-Hohenberg equation

A prototype model in pattern formation is the Swift-Hohenberg equation [41]. This model, originally deduced to describe the pattern formation on Rayleigh-Bénard convection [41], is an isotropic real order parameter nonlinear equation with reflection symmetry.

A recent paper [42], has shown that Alan Turing derived essentially the same equation in a completely different context. In his unpublished draft notes entitled “Outline of the development of the Daisy”, Turing anticipates pattern formation based on the interaction of Fourier modes, proposing the equation and organizing the stability of symmetric pattern solutions through symmetry. As a recognition to both origins of the equation and to emphasize its robustness, from here on we will refer to this model as *the Turing-Swift-Hohenbeg equation*.

A generalization of this equation, including reflection symmetry breaking terms, describes the dynamics of a system in the vicinity of a spatial symmetry breaking instability and close to a second-order critical point marking the onset of a hysteresis loop. This critical point is denominated as the *Lifshitz point* [43]. Due to the universality of this bifurcation, this generalized model has been deduced in several contexts such as chemistry [44], plant ecology [45,46] and nonlinear optics [47].

This model exhibits extended patterns as well as localized structures as equilibrium solutions. However, due to its variational nature, these structures do not have permanent dynamics. In this manuscript, we will consider a non-variational generalization. For a one dimensional spatially extended systems, the model is given by Residori et al. [48], Clerc et al. [49],

$$\partial_t u = \eta + \mu u - u^3 - \nu \partial_{xx} u - \partial_{xxxx} u + 2bu\partial_{xx} u + c(\partial_x u)^2, \quad (1)$$

where  $u = u(x, t)$  is a real scalar field, function of the spatial coordinate  $x$  and time  $t$ . The interpretation of  $u$  depends on the physical context where the model has been derived. For instance, it could correspond to the electric field, deviation of molecular orientations, phytomass density, or chemical concentration [48–50]. Regarding the parameters,  $\mu$  is the bifurcation parameter responsible for the bistability of the homogeneous equilibria. The parameter  $\eta$  is also a bifurcation parameter, breaking the reflection symmetry of the scalar field ( $u \rightarrow -u$ ) and therefore accounts for the asymmetry between homogeneous states. The term proportional to  $\nu$  account of the diffusion ( $\nu < 0$ ) or anti-diffusion process ( $\nu > 0$ ). The symbols  $\partial_{xx}$  and  $\partial_{xxxx}$  stand for the Laplacian and bilaplacian, respectively. The bilaplacian term accounts for a hyper-diffusion process. Terms proportional to  $b$  and  $c$ , account for nonlinear diffusion and advection, respectively. Notice that when  $\eta = b = c = 0$ , one recovers the Turing-Swift-Hohenbeg equation.

### 2.1. Chimera states in continuous media

For a certain region of parameters, model Eq. (1) exhibits coexistence between a chaotic spatiotemporal pattern and a uniform state [23]. In Ref. [51] a detailed study of the chaotic spatiotemporal pattern is reported. As stated before, the coexistence of these behaviors is a prerequisite for observing spatiotemporal chaotic localized states, chaoticons or chimera states in continuous media. A numerical investigation on this parameters region shows that depending on the initial conditions, localized structures of stationary [47], oscillatory [49], and chaotic [23] nature can be observed. Moreover, the width of these localized structures seems to quantify the complexity of their behavior. A wider localized structure allows the existence of a higher number of spatial modes and therefore the number of positive Lyapunov exponents increases [23].

The conducted numerical study considers simulations of model Eq. (1) with periodic boundary conditions. Integration was implemented using a fourth-order explicit Runge-Kutta scheme for the time with a fixed time-step size and a finite differences scheme in space with a centered stencil of 7 grid points.  $dx = 0.6$  and grid size  $L = 400$ . The results presented in this manuscript consider, for the sake of reproducibility, the fixed numerical parameters  $(dt, dx, L) = (0.01, 0.6, 400)$ . We have numerically confirmed that these results hold for different values of the numerical parameters. Likewise, for simplicity, we have only varied the non-variational parameter  $c$  to study chimera states. However, the reported findings are also observed for different values of the other parameters.

Fig. 1 shows a motionless (left panel) and traveling (right panel) chimera-type states observed for the same parameters and different initial conditions. A well-defined speed for the traveling chimera can be observed in the spatiotemporal diagram [cf. Fig. 1(b)]. The motionless (traveling) chimera is characterized on average by being symmetric (asymmetric).

To obtain chimera states, we use as initial conditions asymmetric Gaussians with different widths and heights sustained by the steady homogeneous state. Symmetric and asymmetric Gaussians initial conditions were used for Fig. 1. Chimera states in continuous media can be understood as stable equilibrium points of the interaction of fronts that separate the coherent and incoherent domains [23,24]. They can be considered as attractors and consequently any localized initial condition with size and amplitude similar to a chimera state will converge to it. Consequently, any localized initial condition with size and amplitude similar to a chimera state will converge to it.

To figure out the complexity of motionless and traveling chimera states for the same parameters, we have computed the instantaneous and average power spectrum of each state,  $a[u] \equiv |\int_{-L/2}^{L/2} e^{ikx} u(x, t)|^2 dx$  and  $\langle a[u] \rangle \equiv \int_0^T a[u(t, k)] dt / T$ , respec-

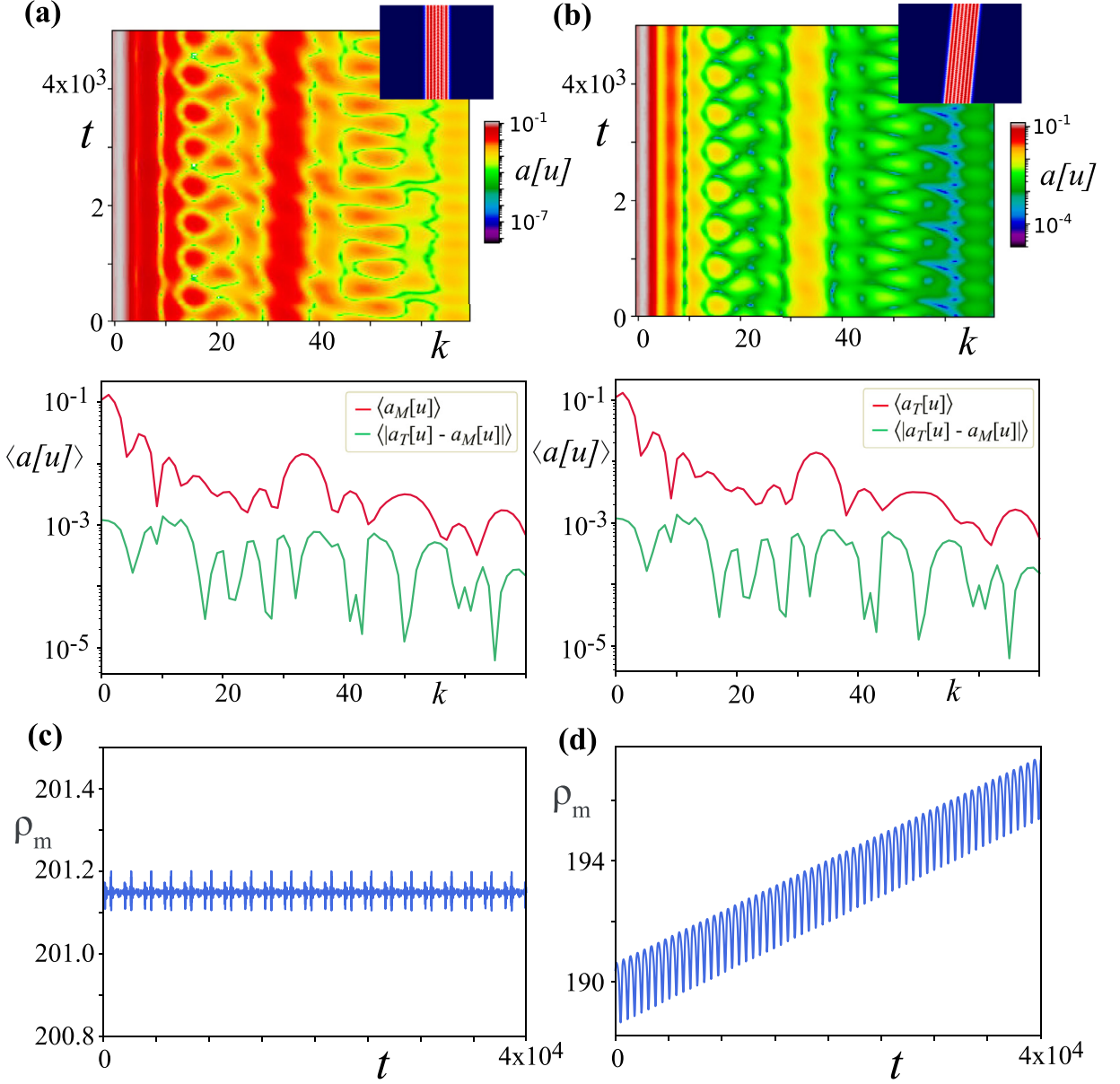


**Fig. 2.** (color online) Motionless versus traveling chimera state. Power spectra of motionless (a) and traveling chimera state (b). The top and bottom panels account for the instantaneous  $a[u]$  and average  $\langle a[u] \rangle$  power spectrum. Insets in top panels stand for spatiotemporal evolution of the motionless and traveling chimera states, respectively. Median evolution of motionless (c) and traveling (d) chimera states.

tively. Fig. 2 depicts the power spectra of motionless and traveling chimera state and the evolution of their median. These spectra reveal the complex spatiotemporal nature of both states. Although the spectra of traveling and motionless chimera share many features, the extra complexity exhibited by the motionless one allows a distinction via the power spectrum (see bottom panels of Fig. 2a and b).

### 3. Propagation characterization of chimera state

To shed light on the collective dynamics of chimera-like states, let us consider as a order parameter, the centroid of the localized structure,

$$\rho_0(t) \equiv \frac{\int_{-L/2}^{L/2} x(u(x,t) - h)dx}{\int_{-L/2}^{L/2} (u(x,t) - h)dx}, \quad (2)$$

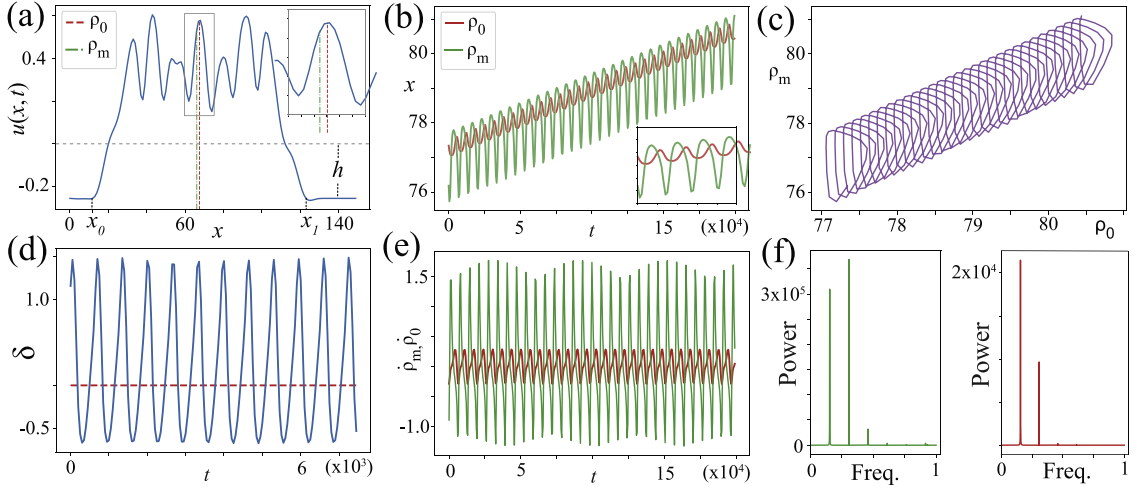


**Fig. 3.** (color online) Propagation characterization of a chimera state for Eq. (1) with  $\eta = -0.04$ ,  $\mu = -0.09$ ,  $\nu = 1$ ,  $b = -1.5$ , and  $c = 10$ . (a) Profile of a propagative chimera-like at a given time. Its centroid  $\rho_0$  and median  $\rho_m$  are indicated by the red and green dashed vertical line, respectively and  $h$  accounts for the background value of the chimera state. (b) Temporal evolution of the centroid and median. (c) Dynamics in the phase portrait build-up by the median and centroid variable. (d) Temporal evolution of the disparity of the localized structure. The dashed curve accounts for the horizontal axis. (e) Temporal derivative of the centroid (green) and median (red). (f) Power spectra of the derivatives of centroid and median, respectively.

where  $L$  is the system size and  $h$  is a constant which corresponds to the background of the chimera state (see Fig. 3a) and statisfy  $\eta + \mu h - h^3 = 0$ . The median of the localized structure is defined by

$$\rho_m(t) \equiv \frac{x_0(t) + x_1(t)}{2}, \quad (3)$$

where  $x_0$  and  $x_1$  are, respectively, the left and right extreme points of the incoherence region (see Fig. 3a). Note that  $u(x_0, t) = u(x_1, t) = -h$ . Fig. 3b shows the temporal evolution of the median (green) and centroid (red) of the chimera state. Both trajectories are oscillating and propagating. The average speed is numerically computed by taking the coefficient of the linear regression fitting for the centroidal trajectory. Fig. 3c depicts the dynamics of the centroid versus the dynamics of the median. Both quantities are oscillating out of phase in the comoving frame. That is, they describe a helicoidal trajectory (a closed cycle in the comoving frame).

To understand the mechanism behind the propagation of chimera states in continuous media, let us introduce the disparity parameter  $\delta(t)$  (or asymmetry) of the localized structure, defined by

$$\delta(t) \equiv \rho_0(t) - \rho_m(t). \quad (4)$$

This quantity measures the asymmetry of the localized solution and a preferential propagation direction will be reflected in the dynamics of  $\delta(t)$ . For instance, Fig. 3(d) depicts the behavior of the disparity. Although this quantity oscillates, the average value is positive and consequently the centroid is shifted towards a direction determined by the initial conditions. Fig. 3(e) provides a speed profile of the localized structure by considering the temporal derivatives of the centroid and median. Power spectra of  $\dot{\rho}_m(t)$  and  $\dot{\rho}_0(t)$  have been included in panel (f), from which we can infer that the dynamic of the centroid and median are anharmonic and they can be represented in good approximation into the dominant Fourier modes.

#### 4. Family of traveling localized structures

To study the family of chimera states and their organization, it will be useful to introduce the following terminology a  $N$ -chimera state corresponds to a chimera with  $N$  peaks.

So far a 7-chimera has been considered. Depending on the initial conditions, given by a slightly asymmetrical Gaussian with several widths were considered. More precisely, we consider widths of the order of 1, 2, 3, ... wavelength of the chaotic spatiotemporal pattern, which allows observing  $N = 6, 7, 8, 9, 10$ , and 11-chimera states. Furthermore, coexistence between distinct propagative chimera states was also observed. Interestingly, the smallest traveling chimera state found in the parameter region considered is a 6-chimera (see Fig. 4a). Fig. 4 shows the spatiotemporal evolution of different traveling chimeras states using the same conventions as Fig. 1. Note that the complexity exhibited by the chimeras seems to increase with their width. As stated before, this can be regarded as a consequence of an increase in the number of positive Lyapunov exponents [23].

For equal parameters, chimera states of larger size propagate faster (have greater mobility). The origin of this is because the engine of propagation is the asymmetry of the localized solution and consequently the larger the localized state, the more asymmetrical modes are involved in the internal dynamics of the chimera solution.

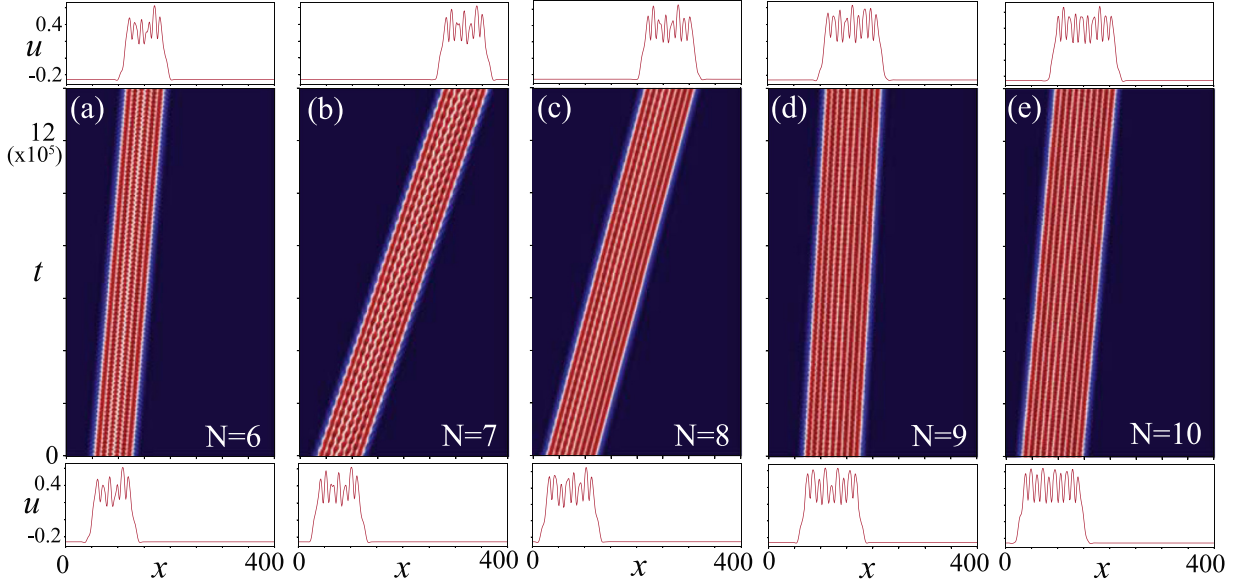


**Fig. 4.** (color online) Spatiotemporal diagrams for diverse traveling chimera states for  $N$ -chimera of model Eq. (1), for  $\eta = -0.04$ ,  $\mu = -0.09$ ,  $\nu = 1$ ,  $b = -1.5$ . (a)  $N = 6$  at  $c = 10.3$ , (b)  $N = 7$  at  $c = 10$ , (c)  $N = 8$  at  $c = 9.7$ , (d)  $N = 9$  at  $c = 9.5$  and (e)  $N = 10$  at  $c = 9.3$ . At the top and bottom of each spatiotemporal diagram is shown the initial ( $t = 0$ ) and final ( $t = 14 \times 10^5$ ) profile state.

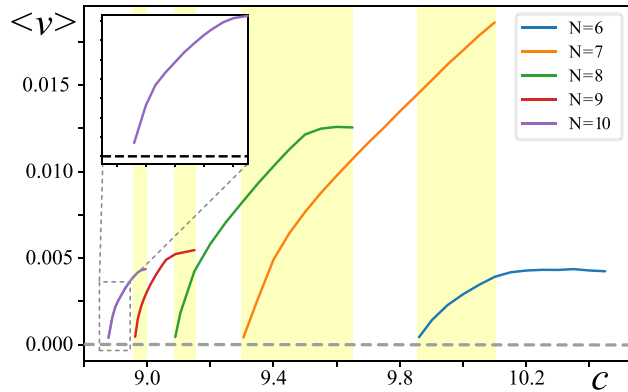


**Fig. 5.** (color online) Average speed  $\langle v \rangle$  and coexistence of traveling chimera states of model Eq. (1) as a function of advection  $c$  parameter, for  $\eta = -0.04$ ,  $\mu = -0.09$ ,  $\nu = 1$ , and  $b = -1.5$ . Painted regions (beige) account for the region of coexistence of two traveling chimera states. The curves of different colors account for localized propagative structures of different peaks. The inset presents more detail of the first branch  $N = 10$ .

To explore the dynamics of a localized solution of a given size, we consider an asymmetric initial condition with a similar size and let the system evolves. Once the solution is stationary, i.e., it maintains its area fluctuating around a value. Then, we determine the centroid and its average speed. By measuring the slope of a linear fit over position with respect to time the average speed is determined. Later, the  $c$  parameter is increased or decreased by  $\pm 0.01$ . To check the persistence of the solution is verified that there are no significant changes in the area and speed. The above process is systematically repeated for different chimeras. Fig. 5 summarizes the speed of chimera states as a function of the non-variational advection parameter  $c$ . Beige panels highlight the regions where coexistence of traveling chimera states is observed. Notice that we have only found regions of a single or coexistence of at most two traveling chimera states. When the value of  $c$  is increased, chimeras propagate faster. Observe that traveling chimera states always emerge with a finite no null speed (see Fig. 5).

Due to the asymmetry generated by the oscillations of the peaks, we conjecture that chimeras smaller than a critical size will not be able to achieve a preferential direction of propagation. Nevertheless, they could still develop an erratic or wandering dynamical behavior within a bounded region of the order of one wavelength. On the other hand, in chimera states of large sizes the centroid is closer to the geometric center on average and therefore the average disparity will tend to zero. Hence, large structures will not propagate. In the parameter regime considered, the largest structure observed was a 11-chimera. Therefore, traveling chimera solutions will only be observed in a range of sizes.

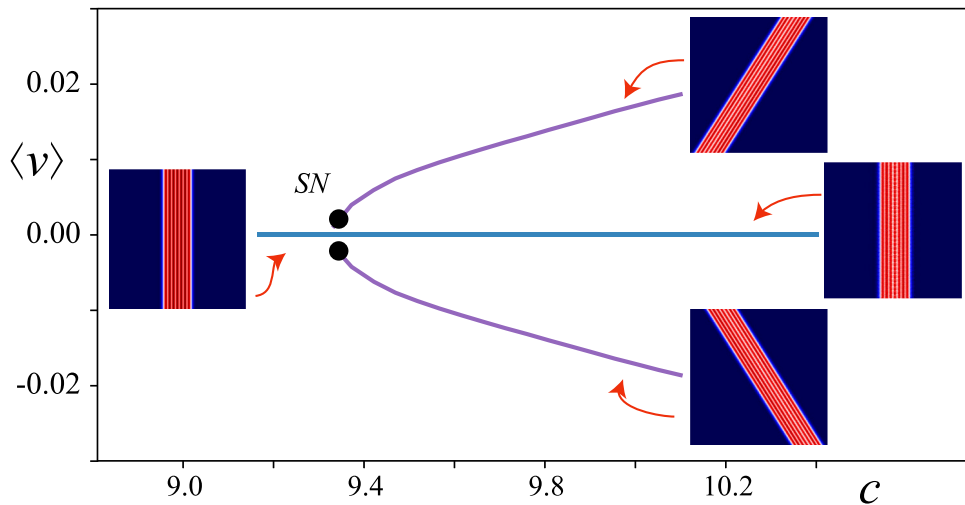


**Fig. 6.** (color online)(a) Speed of 7-chimera states as a function of nonlinear advection parameter  $c$  of model Eq. (1) for  $\eta = -0.04$ ,  $\mu = -0.09$ ,  $\nu = 1$ , and  $b = -1.5$ . The inserts correspond to the respective chimera states. Circles account for the saddle-node bifurcations.

## 5. Bifurcations

In the previous section, we observed that the advection parameter  $c$  in model Eq. (1) seems to control the speed of chimera states. In this section, we consider the transition of a 7-chimera from static to traveling when  $c$  is varied.

Fig. 6 shows the speed of the 7-chimera state as a function of  $c$ . This chart was obtained using a similar method employed for Fig. 5. However, asymmetric and complimentary initial conditions were used to obtain a chimera and its counterpropagating one. The complimentary initial condition is obtained by inverting the spatial coordinate sense. From the numerical simulations we infer that the propagative chimera states emerge from a saddle-node bifurcation. This instability is represented by full circles denoted by SN in Fig. 6. Due to the lack of a continuation method for unstable chaotic solutions, we can not complete the bifurcation diagram. By increasing the value of parameter  $c$ , we observe that the propagative chimera becomes unstable. Depending on the initial conditions, this propagative localized states can engender the uniform state, smaller localized structures, or motionless chimera. Therefore, the basin of attraction of these equilibria are of complex nature, probably with fractal structures. Studies of these basins of attraction are in progress.

## 6. Conclusions

We have shown a novel class of chimera traveling solutions in spatially extended continuous systems, using the non-variational Turing-Swift-Hohenberg type Eq. (1), as a prototype model. Since this is a model of broad interest in pattern formation and relevant in a wide variety of systems [50], we expect to observe these solutions in several natural and technological systems.

We have investigated the properties of chimera states by defining and studying the temporal evolution of the centroid and median of localized structures. These quantities suggested the consideration of the disparity to measure the asymmetry of chimeras in time. The disparity provided a description for the mechanism responsible for the propagation of chimera states. In particular, it provides a plausible argument for the existence of traveling chimera state in an interval of sizes (6–11 in our case). Moreover, using this dynamical quantities a bifurcation diagram of stable propagative chimera solutions has been presented. To obtain a complete bifurcation diagram, a continuation method is required. However, there are not continuation methods for unstable chaotic solutions yet. This is a major problem in modern bifurcation theory.

Recently, the chimera state phenomenon has been extended to 2 and 3 spatial dimensions [25,26,32,52–55]. We expect that the phenomenon studied in the present paper can be observed in more dimensions, work in this direction is in progress.

## Declaration of Competing Interest

The authors declare that they have no known competing financial interests or personal relationships that could have appeared to influence the work reported in this paper.

## CRediT authorship contribution statement

**A.J. Alvarez-Socorro:** Conceptualization, Investigation, Validation, Software, Writing - original draft, Writing - review & editing. **M.G. Clerc:** Supervision, Project administration, Conceptualization, Investigation, Validation, Methodology, Writing - review & editing. **N. Verschueren:** Writing - review & editing, Validation.

## Acknowledgments

MGC thanks for the financial support of FONDECYT projects 1180903. This work was funded by ANID–Millennium Science Initiative Program–ICN17\_012. AJAS thanks financial support from Becas Conicyt 2015, Contract no. 21151618.

## References

- [1] Kaneko K. Clustering, coding, switching, hierarchical ordering, and control in a network of chaotic elements. *Phys D* 1990;41:137–72.
- [2] Kuramoto Y, Battogtokh D. Coexistence of coherence and incoherence in nonlocally coupled phase oscillators. *Nonlinear Phenom Complex Syst* 2002;5:380–5.
- [3] Abrams DM, Strogatz SH. Chimera states for coupled oscillators. *Phys Rev Lett* 2004;93:174102.
- [4] Tinsley MR, Nkomo S, Showalter K. Chimera and phase-cluster states in populations of coupled chemical oscillators. *Nat Phys* 2012;8:662–5.
- [5] Hagerstrom AM, Murphy TE, Roy R, Hövel P, Omelchenko I, Schöll E. Experimental observation of chimeras in coupled-map lattices. *Nat Phys* 2012;8:658–61.
- [6] Omel'chenko OE. Coherence-incoherence patterns in a ring of non-locally coupled phase oscillators. *Nonlinearity* 2013;26:2469–98.
- [7] Martens EA, Thutupalli S, Fourrier A, Hallatschek O. Chimera states in mechanical oscillator networks. *Proc Natl Acad Sci* 2013;110:10563.
- [8] Kapitaniak T, Kuzma P, Wojewoda J, Czolczynski K, Maistrenko Y. Imperfect chimera states for coupled pendula. *Sci Rep* 2014;4:6379.
- [9] Gambuzza LV, Buscarino A, Chessa S, Fortuna L, Meucci R, Frasca M. Experimental investigation of chimera states with quiescent and synchronous domains in coupled electronic oscillators. *Phys Rev E* 2014;90:032905.
- [10] Larger L, Penkovsky B, Maistrenko Y. Virtual chimera states for delayed-feedback systems. *Phys Rev Lett* 2013;111:054103.
- [11] Wickramasinghe M, Kiss IZ. Spatially organized dynamical states in chemical oscillator networks: synchronization, dynamical differentiation, and chimera patterns. *PLoS One* 2013;8:e80586x.
- [12] Schmidt L, Schönleber K, Krischer K, Garcia-Morales V. Coexistence of synchrony and incoherence in oscillatory media under nonlinear global coupling. *Chaos* 2014;24:013102.
- [13] Wickramasinghe M, Kiss IZ. Spatially organized partial synchronization through the chimera mechanism in a network of electrochemical reactions. *Phys Chem Chem Phys* 2014;16:18360.
- [14] Rosin DP, Rontani D, Haynes ND, Schöll E, Gauthier DJ. Transient scaling and resurgence of chimera states in networks of boolean phase oscillators. *Phys Rev E* 2014;90:030902(R).
- [15] Clerc MG, Coulibaly S, Ferre MA, Garcia-Nustes MA, Rojas RG. Chimera-type states induced by local coupling. *Phys Rev E* 2016;93:052204.
- [16] Hizanidis J, Lazarides N, Tsironis GP. Robust chimera states in SQUID metamaterials with local interactions. *Phys Rev E* 2016;94:032219.
- [17] Clerc M, Ferré MA, Coulibaly S, Rojas RG, Tlidi M. Chimera-like states in an array of coupled-waveguide resonators. *Opt Lett* 2017;42:2906–9.
- [18] Clerc MG, Coulibaly S, Ferré MA, Rojas RG. Chimera states in a duffing oscillators chain coupled to nearest neighbors. *Chaos* 2018;28:083126.
- [19] Compte A, Brunel N, Rakic GPS, Wang XJ. Synaptic mechanisms and network dynamics underlying spatial working memory in a cortical network model. *Cerebral Cortex* 2000;10:910–23.
- [20] Larger L, Penkovsky B, Maistrenko Y. Laser chimeras as a paradigm for multistable patterns in complex systems. *Nat Commun* 2015;6:7752.
- [21] Viktorov EA, Habruseva T, Hegarty SP, Huyet G, Kelleher B. Coherence and incoherence in an optical comb. *Phys Rev Lett* 2014;112:224101.
- [22] Uy CH, Weicker L, Rontani D, Sciamanna M. Optical chimera in light polarization. *APL Photon* 2019;4:056104.
- [23] Verschueren N, Bortolozzo U, Clerc MG, Residori S. Spatiotemporal chaotic localized state in liquid crystal light valve experiments with optical feedback. *Phys Rev Lett* 2013;110:104101.
- [24] Verschueren N, Bortolozzo U, Clerc MG, Residori S. Chaoticon: localized pattern with permanent dynamics. *Philos Trans R Soc A* 2014;372:20140011.
- [25] Schmidt L, Krischer K. Chimeras in globally coupled oscillatory systems: From ensembles of oscillators to spatially continuous media. *Chaos* 2015;25:064401.
- [26] Nicolaou ZG, Riecke H, Motter AE. Chimera states in continuous media: Existence and distinctness. *Phys Rev Lett* 2017;119:244101.
- [27] Alvarez-Socorro AJ, Clerc MG, Ferré M. Wandering walk of chimera-like states in continuous media. Manuscript submitted for publication 2020.
- [28] Bohr T, Jensen MH, Paladin G, Vulpiani A. Dynamical systems approach to turbulence. Cambridge University Press; 2005.
- [29] Pomeau Y. Front motion, metastability and subcritical bifurcations in hydrodynamics. *Phys D* 1986;23:3–11.
- [30] Coullet P, Riera C, Tresser C. Stable static localized structures in one dimension. *Phys Rev Lett* 2000;84:3069.
- [31] Dudkowski D, Czolczyński K, Kapitaniak T. Traveling chimera states for coupled pendula. *Nonlinear Dyn* 2019;95:1859–66.
- [32] Omel'chenko OE. Traveling chimera states. *J Phys A* 2019;52:104001.
- [33] Xie J, Knobloch E, Kao HC. Multicenter and traveling chimera states in nonlocal phase-coupled oscillators. *Phys Rev E* 2014;90:022919.
- [34] Omel'chenko O, Wolfrum M, Maistrenko YL. Chimera states as chaotic spatiotemporal patterns. *Phys Rev E* 2010;81:065201(R).
- [35] Turaev D, Radziunas M, Vladimirov AG. Chaotic soliton walk in periodically modulated media. *Phys Rev E* 2008;77:065201(R).
- [36] Zambrini R, Papoff F. Signal amplification and control in optical cavities with off-axis feedback. *Phys Rev Lett* 2007;99:063907.
- [37] Staliunas K, Sanchez-Morcillo VJ. Spatial-localized structures in degenerate optical parametric oscillators. *Phys Rev A* 1998;57:1454–7.
- [38] Haudin F, Rojas RG, Bortolozzo U, Clerc MG, Residori S. Vortex emission accompanies the advection of optical localized structures. *Phys Rev Lett* 2011;106:063901.
- [39] Alvarez-Socorro AJ, Clerc MG, Tlidi M. Spontaneous motion of localized structures induced by parity symmetry breaking transition. *Chaos* 2018;28:053119.
- [40] Alvarez-Socorro AJ, Clerc M, Gonález-Cortés G, Wilson M. Nonvariational mechanism of front propagation: Theory and experiments. *Phys Rev E* 2017;95:010202.
- [41] Swift J, Hohenberg PC. Hydrodynamic fluctuations at the convective instability. *Phys Rev A* 1977;15:319–28.
- [42] Dawes JH. After 1952: the later development of Alan Turing's ideas on the mathematics of pattern formation. *Hist Math* 2016;43:49–64.
- [43] Hornreich RM, Luban M. Critical behavior at the onset of  $k$ -space instability on the  $\lambda$  line. *Phys Rev Lett* 1975;35:1678–82. R. M. Hornreich, *J. Magn. Magn. Mater.* 1980; 15, 387.
- [44] Hilali MF, Dewel G, Borckmans P. Subharmonic and strong resonances through coupling with a zero mode. *Phys Lett A* 1996;217:263–8.
- [45] Tlidi M, Lefever R, Vladimirov A. On vegetation clustering, localized bare soil spots and fairy circles. *Lect Notes Phys* 2008;751:381–402.
- [46] Lefever R, Barbier N, Couderon P, Lejeune O. Deeply gapped vegetation patterns: on crown/root allometry, criticality and desertification. *J Theor Biol* 2009;261:194–209.
- [47] Tlidi M, Mandel P, Lefever R. Localized structures and localized patterns in optical bistability. *Phys Rev Lett* 1994;73:640–3.
- [48] Residori S, Petrossian A, Nagaya T, Clerc MG. Localized structures and their dynamics in a liquid crystal light valve with optical feedback. *J Opt B* 2004;6:S169.
- [49] Clerc MG, Petrossian A, Residori S. Bouncing localized structures in a liquid-crystal light-valve experiment. *Phys Rev E* 2005;71:015205(R).
- [50] Kozyreff G, Tlidi M. Nonvariational real Swift-Hohenberg equation for biological, chemical, and optical systems. *Chaos* 2007;17:037103.
- [51] Clerc MG, Verschueren N. Quasiperiodicity route to spatiotemporal chaos in one-dimensional pattern-forming systems. *Phys Rev E* 2013;88:052916.
- [52] Maistrenko Y, Sudakov O, Osiv O, Maistrenko V. Chimera states in three dimensions. *New J Phys* 2015;17.
- [53] Laing CR. Chimeras in two-dimensional domains: heterogeneity and the continuum limit. *SIAM J Appl Dyn Syst* 2017;16:974.
- [54] Omel'chenko OE, Knobloch E. Chimerapedia: coherence–incoherence patterns in one, two and three dimensions. *New J Phys* 2019;21:093034.
- [55] Clerc MG, Coulibaly S, Ferre N, Tlidi M. Two-dimensional optical chimera states in an array of coupled waveguide resonators. *Chaos* 2020;30:043107.